

Polarimetric Observations of the Masers in NGC 4258: An Upper Limit on the Large-Scale Magnetic Field 0.2 pc from the Central Engine

J.R. Herrnstein¹, J.M. Moran, L.J. Greenhill

Harvard-Smithsonian Center for Astrophysics, Mail Stop 42, 60 Garden Street, Cambridge, MA 02138

E.G. Blackman

Institute of Astronomy, Madingley Road, Cambridge, CB3 0HA

and P.J. Diamond

National Radio Astronomy Observatory, PO Box 0, Socorro, NM 87801

ABSTRACT

We report VLA 1σ upper limits of 1.5% and 3% on the intrinsic circular and linear fractional polarizations, respectively, of the water vapor maser emission 0.2 pc from the central engine of NGC 4258. A corresponding 0.5% upper limit on any Zeeman-splitting-induced circular polarization translates to a 1σ upper limit on the parallel, or toroidal, component of the magnetic field of 300 mG. Assuming magnetic and thermal pressure balance in the disk, this magnetic field upper limit corresponds to a model-dependent estimate of the accretion rate through the molecular disk of $10^{-1.9}\alpha M_{\odot} \text{ yr}^{-1}$ for the case where the magnetic field lies along the line of sight.

Subject headings: accretion, accretion disks — galaxies: individual, NGC 4258 — galaxies: nuclei — magnetic fields — masers — polarization

1. Introduction

Active galactic nuclei (AGN) are thought to be powered by accretion onto a central, supermassive black hole (e.g. Rees 1984) and it is probable that magnetic fields play an important role in this process. They are often invoked as a potential source of viscosity and

¹Current Address: National Radio Astronomy Observatory, PO Box 0, Socorro, NM 87801

therefore dissipation and angular momentum transport in the accretion flow (c.f. Balbus & Hawley 1991). In addition, large-scale magnetic fields may be important in the energetics, collimation, and confinement of jets and broad line regions (Blandford & Payne 1982; Emmering, Blandford & Shlosman 1992). Finally, the typical broad-band AGN spectrum is not adequately fit by a simple blackbody law, and many of the proposed non-thermal radiation processes require a substantial magnetic field.

Magnetic field strengths can be estimated from radio observations in a variety of ways. For example, if the source size can be estimated, then a determination of the synchrotron turnover frequency yields an estimate for the field strength. Alternatively, if the gas density can be estimated, then Faraday rotation measurements can also provide reasonably accurate field strengths. But the most direct method for estimating magnetic field strengths is via observations of the Zeeman splitting of spectral lines of various atomic and molecular species in regions of high density neutral gas. Unfortunately, for gas in thermal equilibrium it is impossible to apply this technique to AGN, as the interferometers needed to resolve the central engines of AGN have insufficient sensitivity to study the low surface brightness neutral gas emission where the Zeeman splitting occurs. However, the extreme non-thermal equilibrium conditions characteristic of extragalactic masers offer an unusual opportunity to measure AGN magnetic fields. To date approximately 21 H₂O megamasers and 50 OH megamasers have been detected in the nuclei of nearby AGN (e.g. Braatz, Wilson & Henkel 1997). They are often several orders of magnitude more luminous than Galactic masers, and many are bright enough to be studied with VLBI.

NGC 4258 is a mildly active Seyfert 2 galaxy with a 2–10 keV X-ray luminosity of 4×10^{40} erg s⁻¹ and an obscuring column of 1.5×10^{23} cm⁻² (Makishima *et al.* 1994). Nuclear continuum and narrow line emission are seen in reflected, polarized optical light (Wilkes *et al.* 1995). The galaxy harbors an H₂O maser (Claussen, Heiligman, & Lo 1984), and VLBA observations reveal that the maser traces an extremely thin, slightly warped, nearly edge-on disk in the nucleus of the galaxy (Watson & Wallin 1994; Greenhill *et al.* 1995; Miyoshi *et al.* 1995; Moran *et al.* 1995; Herrnstein, Greenhill, & Moran 1996). The masers are 0.13–0.26 pc from the center of mass of the disk, assuming a distance of 6.4 Mpc. The nearly perfect Keplerian rotation curve of the masers requires a central mass of $3.5 \times 10^7 M_{\odot}$ within 0.13 pc. The velocity centroid of the disk is consistent with the optical systemic velocity of the galaxy and the rotation axis of the disk is well-aligned with a 100-pc-scale radio jet (Cecil, Wilson, & De Pree 1995). VLBA observations also reveal subparsec-scale jet emission along the disk axis (Herrnstein *et al.* 1997). Deguchi, Nakai, & Barvainis (1995) report an upper limit on the linear polarization of about 20% for the highly Doppler-shifted masers and about 15% for those features near the galaxy’s systemic velocity.

Here, we report an attempt to measure the Zeeman splitting of an isolated, strong maser feature in the sub-parsec-scale disk of NGC 4258 using VLA polarimetric observations. The observations are discussed in Section 2, and the results are interpreted in Section 3. Section 4 considers the implications of the measurements.

2. Observations

The positions and line-of-sight (LOS) velocities of the masers in NGC 4258 define a nearly edge-on, slightly warped disk, which is shown in the top portion of Figure 1. The figure also includes a VLBA spectrum of the red-shifted maser emission. The dashed vertical lines in this spectrum show the frequency range observed in the current observation. We chose to observe the feature 0.2 pc from the center of mass with a LOS velocity of 1306 km s^{-1} because it is fairly isolated and has remained strong since it was first detected by Nakai, Inoue, & Miyoshi (1993). Because the feature lies approximately along the intersection of the disk with the plane of the sky and because the disk is inclined to the LOS by $\lesssim 8^\circ$, all subsequent references to B_{\parallel} correspond to any toroidal fields that may be present in the disk, while references to the perpendicular component of the field (B_{\perp}) concern either vertical or radial fields.

The 1306 km s^{-1} feature was observed for 12 hours on 1995 October 20/21 with the B-configuration VLA of the NRAO.² The skies were clear for the first 8 hours, but became progressively overcast during the final 4 hours. A bandwidth of 1.56 MHz was observed and correlated in full polarization mode with 128 channels and uniform weighting, and the resulting 0.19 km s^{-1} velocity resolution provided about six channels across the maser line. Bandpass, amplitude, and phase calibration were performed in AIPS using standard techniques. We were able to self-calibrate the 1306 km s^{-1} feature for the first 8 hours of the experiment. Linear polarization calibration was performed in two steps. First, a strong, source (OJ287) was observed over a broad range of parallactic angle in order to quantify any discrepancies in the polarization responses of the antenna feeds. Second, a strongly polarized source with known polarization angle (3C286) was observed to determine the intrinsic phase difference between the left and right channels. After imaging, the amplitude calibration was refined by fitting Gaussians to the 1306 km s^{-1} feature and renormalizing the left and right circular polarizations (LCP and RCP) to yield equal integrated line strengths. This procedure removes any intrinsic circular polarization from the data and makes possible

²The National Radio Astronomy Observatory is a facility of the National Science Foundation operated under cooperative agreement by Associated Universities, Inc.

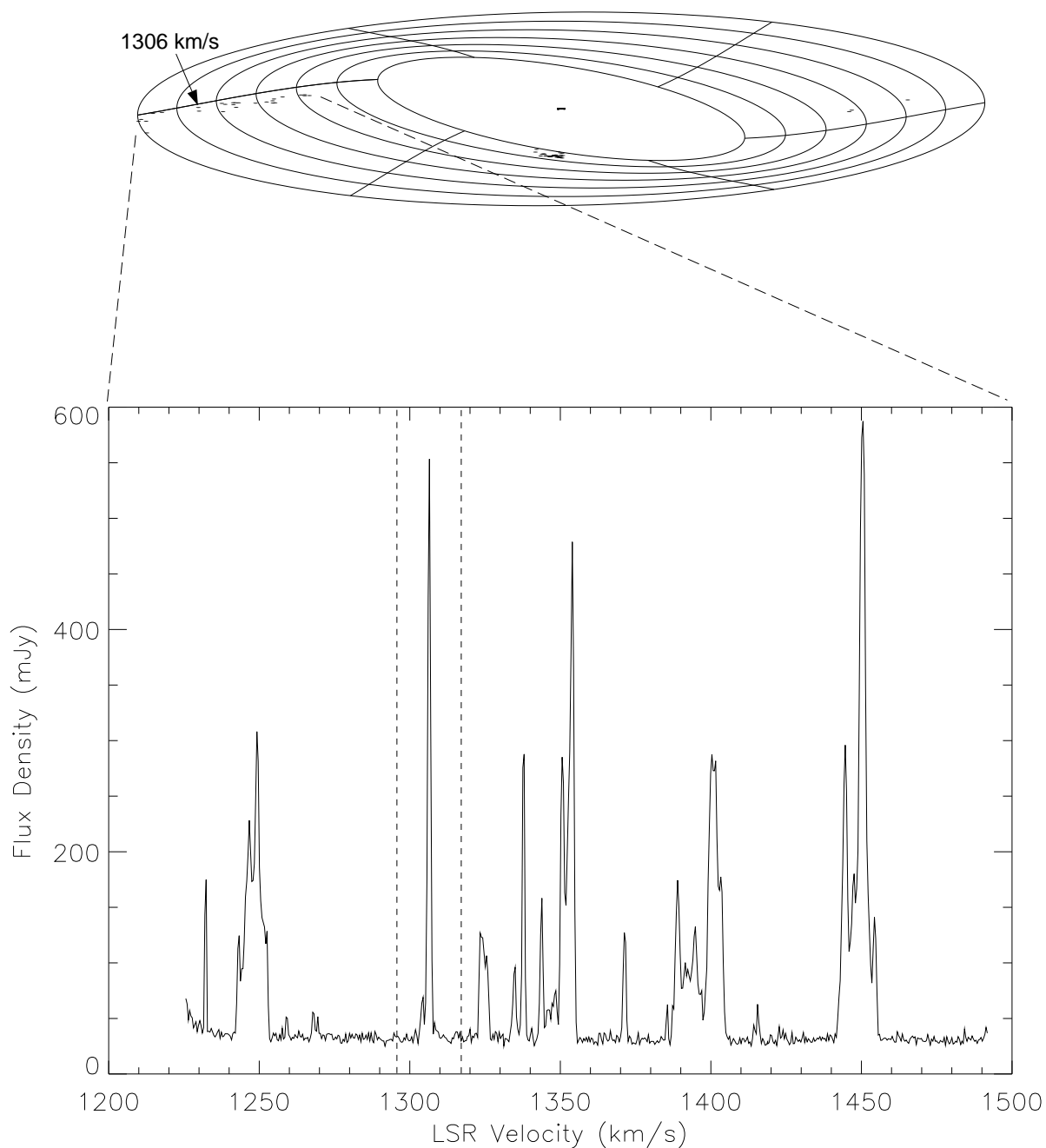


Fig. 1.— *Top*: The best-fitting warped disk model in NGC 4258 (Herrnstein 1997), with the maser features superposed. The disk has been tipped down 10° from its true orientation to make the masers more visible. *Bottom*: Spectrum of the red-shifted maser features. The data were taken with the VLBA on 29 May, 1995 (Herrnstein 1997). The frequency range observed for the current work is indicated by the dashed vertical lines.

the detection of any Zeeman-splitting-induced circular polarization. The renormalization factor was about 0.99, which suggests there is no intrinsic circularly polarized emission (with a spectral profile similar to that of the Stokes I profile) to a limit of about 1 percent of the total flux in the line.

The results are summarized in Figure 2. The top panel shows the full 128-channel Stokes I ($\equiv 1/2[\text{LCP} + \text{RCP}]$) synthesized spectrum, with a thermal noise of about 6 mJy per channel. Comparison with Figure 1 shows that the flux density of the 1306 km s^{-1} feature has remained steady at approximately 0.5 Jy over the 6-month time baseline. The best fitting Gaussian is centered at 1306.4 km s^{-1} (LSR, radio definition) and has a line width, σ_v , of 0.49 km s^{-1} (FWHM, Δv , of 1.15 km s^{-1}). We note that the actual deconvolved FWHM is about 1.13 km s^{-1} . The Stokes V ($\equiv 1/2[\text{LCP} - \text{RCP}]$) spectrum is shown in the middle panel of Figure 2, while the bottom panel shows the total linear polarization spectrum (Stokes $\sqrt{Q^2 + U^2}$). *There is no evidence for any intrinsic polarization in the 1306 km s^{-1} maser feature, and we report 1σ upper limits of 1.5% and 3% on the fractional circular (V/I) and linear polarizations, respectively.*

3. Interpretation

An external magnetic field, \vec{B} , induces a precession in the magnetic moment of the water molecule about \hat{B} . The energy of this precession generates magnetic sublevels (M_F) by lifting the degeneracy within the hyperfine states of water. Zeeman splitting arises from transitions between these sublevels, according to the selection rule $\Delta M_F = 0, \pm 1$. The $\Delta M_F = \pm 1$ transitions give rise to line emission asymmetrically shifted in frequency from the hyperfine transition rest frequency, and possessing counter-rotating circular polarizations in the plane perpendicular to \hat{B} . Because water is non-paramagnetic, \vec{B} couples primarily to the nuclear magnetic dipole moment of the molecule, and the splitting of the left and right circular polarizations ($\Delta\nu_z$) is only about 10 Hz mG^{-1} (c.f. Feibig & Güsten 1989; hereafter FG). Thus, for mG-level magnetic fields the Zeeman splitting is 10^{-3} – 10^{-4} times narrower than typical water maser linewidths. For such fractional Zeeman splitting, the Stokes V spectrum is well-approximated as the first derivative of the total power spectrum, I, times the splitting width:

$$V(v) \simeq \frac{dI}{dv} \Delta v_z = \frac{I_o \Delta v_z}{\sigma_v^2} v e^{-\frac{v^2}{2\sigma_v^2}}, \quad (1)$$

where we have modeled the line as a Gaussian with amplitude I_o , and where Δv_z is the Zeeman splitting in units of velocity and v is the offset from line center in velocity. Equation 1 is an antisymmetric sinusoid, or “S-curve” with extrema of $\pm e^{-1/2} I_o \Delta v_z / \sigma_v$ at

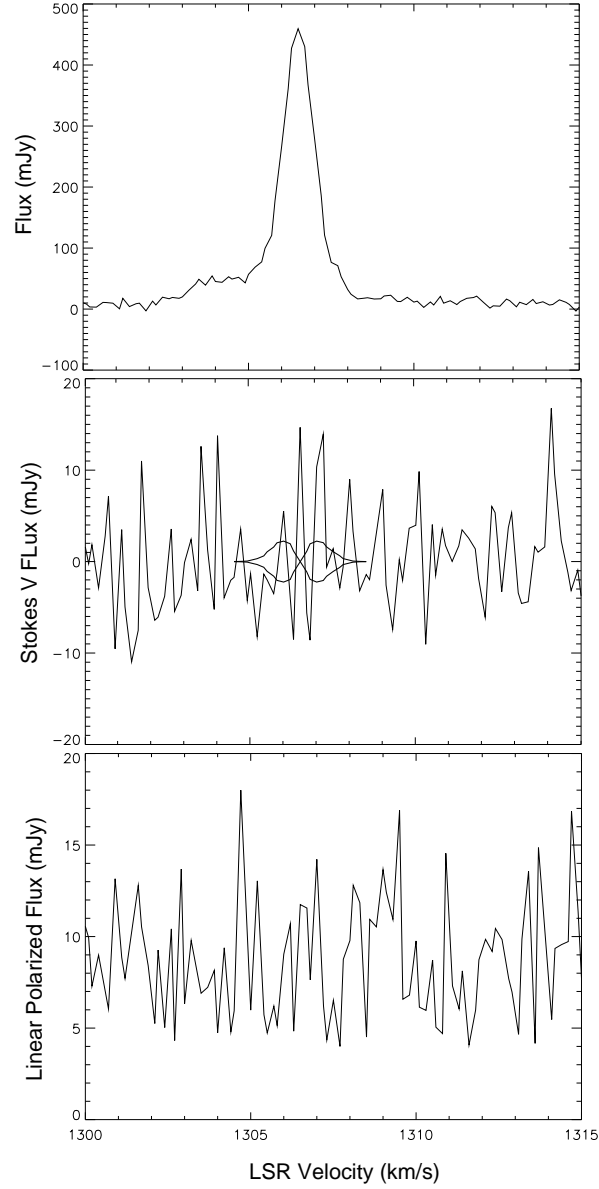


Fig. 2.— VLA polarimetry of the NGC 4258 maser feature at 1306 km s^{-1} . *Top*: Stokes I spectrum. *Middle*: Stokes V spectrum, with the $\pm 1\sigma$ Zeeman S-spectra superposed. *Bottom*: Total linear polarization spectrum.

$v = \pm\sigma_v$. Note that the spectrum need only be sampled at a fraction of σ_v , as opposed to a fraction of Δv_z , in order to detect the Zeeman splitting.

In practice, the Zeeman pattern of H₂O is more complex since in the presence of a magnetic field the 7–6, 6–5, and 5–4 hyperfine transitions that dominate the water maser spectrum are themselves comprised of 13, 11, and 9 different lines in each polarization, each with its own characteristic Δv_z . FG have modelled the theoretical H₂O Zeeman pattern, and they find that the S-curve extrema (V_{max}) are approximately given by

$$\frac{V_{max}}{I_o} \simeq A_{F-F'} \frac{B_{\parallel} \text{ [G]}}{\Delta v \text{ [km s}^{-1}\text{]}}, \quad (2)$$

where $A_{F-F'}$ equals 0.0133, 0.0083, and 0.001 km s^{−1} G^{−1} for the 7-6, 6-5, and 5-4 transitions, respectively. Polarimetric observations of H₂O masers interpreted with equation 1 and normalized according to equation 2 have been used to infer interstellar magnetic fields of up to 100 mG in galactic star formation regions (FG; Zhao, Goss, & Diamond 1992). FG find that the magnetic fields measured using Zeeman splitting correlate well with density in molecular clouds over several orders of magnitude. This is consistent with expectations based on flux freezing arguments, and provides circumstantial support for the validity of the Zeeman technique.

Equations 1 and 2 neglect the unusual radiative transfer properties and nonthermal nature of masers. Nedoluha & Watson (1992) explore the validity of the FG S-curve formulation for fractional Zeeman splitting in light of the full transfer equations and considering all hyperfine transitions. Their numerical simulations verify the standard Zeeman splitting methodology in the regime of mild maser saturation and suggest that $A_{F-F'} = 0.020 \text{ km s}^{-1} \text{ G}^{-1}$ accurately accounts for all hyperfine transitions taken together. For extreme saturation, effects such as line re-broadening and non-Maxwellian particle velocities may become significant, limiting the precision of the magnetic field estimates to factors of a few. In addition, as the stimulated emission rate, R , approaches Δv_z for highly saturated masers, strong “false” circular polarizations can be induced that are similar in form to the Zeeman pattern, and therefore conducive to *overestimates* of the magnetic field (Nedoluha & Watson 1990).

The results of the numerical simulations emphasize that the degree of saturation is important in interpreting maser polarization observations. For a cylindrical maser (c.f. Reid and Moran 1988)

$$R \simeq 8 \left[\frac{S_{\nu}}{1 \text{ Jy}} \right] \left[\frac{l}{10^{-2} \text{ pc}} \right]^{-2} \left[\frac{d}{6.4 \text{ Mpc}} \right]^2 \text{ s}^{-1}. \quad (3)$$

where S_{ν} and l are the flux density and length of the maser, respectively, and d is the distance to the source. A maser becomes saturated when R surpasses Γ , the relaxation rate

from the maser levels, which is usually assumed to be $\lesssim 1 \text{ s}^{-1}$ for the relevant levels of the water molecule. In NGC 4258, both velocity coherence and beam angle arguments suggest $l \lesssim 0.002 \text{ pc}$ for the high-velocity masers (Moran *et al.* 1995). Therefore, $R \gtrsim 10^2 \text{ s}^{-1}$ for the $\sim 0.5 \text{ Jy}$ feature at 1306 km s^{-1} , and the maser is probably highly saturated. We note that the 1.1 km s^{-1} FWHM of the line is consistent with that of a re-broadened, highly saturated maser at $\sim 300 \text{ K}$ (Nedoluha & Watson 1991).

We derive an upper limit on B_{\parallel} from the observed Stokes V spectrum using equations 1 and 2 with $A_{F-F'} = 0.020 \text{ km s}^{-1} \text{ G}^{-1}$ and $\Delta v = 1.15 \text{ km s}^{-1}$. A χ^2 minimization procedure in which B_{\parallel} is the only free parameter indicates that $V_{\text{max}} \lesssim 2.2 \text{ mJy}$ and $|B_{\parallel}| \lesssim 300 \text{ mG}$ (1σ). Here, B_{\parallel} represents any toroidal component of the magnetic field at 0.2 pc radius that is not significantly tangled across the maser. The $\pm 300 \text{ mG}$ Zeeman S-curve corresponding to the upper limit on B_{\parallel} are included in the middle panel of Figure 2. If the maser line consists of only the 7–6 hyperfine component, as is commonly assumed, then the field strength limit would be about 50% higher. Finally, we note that if the maser is indeed highly saturated, the upper limit is uncertain by factors of a few.

Interpreting the linear polarization upper limit is more difficult, as there is substantial uncertainty surrounding the theory of linear polarization in masers exposed to an external magnetic field (c.f. Deguchi & Watson 1990; Elitzur 1996). In general, the degree of linear polarization will probably depend quite strongly on the saturation state of the maser (Goldreich, Keeley, & Kwan 1973; Nedoluha & Watson 1992), and this injects considerable uncertainty into field strength estimates based on linear polarization observations. Furthermore, it is difficult to quantify the degree to which the linear polarization observations have been affected by Faraday depolarization within the maser itself, since the ionization fraction and number density (n) in the molecular layer of the disk are both rather uncertain. For $n \sim 10^{10} \text{ cm}^{-3}$, a magnetic field of 300 mG , and a maser length of 0.002 pc , a fractional ionization as low as 10^{-8} would lead to significant Faraday depolarization (Thompson, Moran, & Swenson 1986). We note that a recent analysis of circumstellar SiO masers suggests that Faraday depolarization is not important in such systems (Wallin & Watson 1997). However, in the present analysis we will refrain from translating the 3% upper limit on the linear polarization into an upper limit on the magnetic field.

4. Discussion and Future Prospects

The upper limit on the magnetic field at 0.2 pc radius can be compared to a second upper limit relating to pressure balance in the disk. Moran *et al.* (1995) use the scatter in

the vertical component of the systemic masers to place an upper limit of 0.0003 pc on the scale height, H , of the maser layer. If the disk is supported by magnetic pressure and is in hydrostatic equilibrium then $H/r = v_A/v_\phi$, where r is the radius, v_A is the Alfvén velocity ($v_A = B/\sqrt{4\pi\rho}$), and v_ϕ is the Keplerian rotation velocity. ρ is the density in the maser layer, and the Alfvén velocity in question relates to any magnetic field geometry capable of supplying pressure in the vertical direction: tangled, radial, and toroidal fields all suffice. We require $n \lesssim 10^{10} \text{ cm}^{-3}$ in order to support maser action and conclude that $B \lesssim 80 \text{ mG}$ in the maser layer at $r = 0.2 \text{ pc}$, the equality holding for a magnetically dominated disk characterized by the quoted upper limits for thickness and density. The 300 mG upper limit on B_\parallel provided by the Zeeman analysis does not preclude a magnetically supported disk. It does, however, provide a more robust upper limit on the field strength than do hydrostatic equilibrium considerations, since the masers could in principle be sampling a thin layer in a much thicker disk.

NGC 4258 is an exceptional laboratory for the study of AGN accretion processes. The nuclear maser reveals details about the kinematics and structure of the accretion disk on sub-parsec scales and permits the determination of the central mass with great precision. In addition to being constrained by these observations, efforts to construct self-consistent models of the accretion in NGC 4258 must necessarily address the fact that the central engine luminosity (L) is extremely sub-Eddington: ($L \sim 10^{42\pm 1} \text{ ergs}^{-1} = 10^{-3.6\pm 1} L_E$; Herrnstein *et al.* 1998). Neufeld & Maloney (1995) demonstrate that for an accretion rate, \dot{M} , of approximately $10^{-4.1}\alpha \text{ M}_\odot \text{ yr}^{-1}$, the molecular disk becomes atomic throughout for radii greater than about 0.26 pc, thereby providing a physical explanation for the observed outer limit of the maser emission. Here, α is the standard Shakura-Sunyaev parameterization of the kinematic viscosity. This accretion rate corresponds to a radiative efficiency of $10^{-0.6\pm 1}\alpha^{-1}$ and suggests that NGC 4258 is powered by a highly efficient, but mass-starved, optically thick, geometrically thin accretion disk (Shakura & Sunyaev 1973). Alternatively, Lasota *et al.* (1996) have proposed that NGC 4258 is powered by a central geometrically thick, optically thin advection-dominated accretion flow (ADAF; Narayan & Yi 1995a&b). In this scenario, the vast majority of viscously dissipated energy is deposited into an extremely hot ($\sim 10^{12} \text{ K}$), largely non-radiative proton plasma, and the low luminosity of the system is due to low radiative efficiencies as opposed to mass starvation of the central black hole. In the ADAF models the broad-band spectrum, from radio to hard X-ray, is the result of various nonthermal processes in a relatively cool ($\sim 10^{9.5} \text{ K}$) electron plasma. Lasota *et al.* (1996) fit the optical and X-ray NGC 4258 emission with an $\dot{M} \simeq 10^{-1.9}\alpha \text{ M}_\odot \text{ yr}^{-1}$ ADAF. More recent calculations by Narayan (personal communication), suggest $\dot{M} \simeq 10^{-1.7}\alpha \text{ M}_\odot \text{ yr}^{-1}$, corresponding to a radiative efficiency of $10^{-3\pm 1}\alpha^{-1}$. We note that recent high-resolution radio continuum observations

suggest that if NGC 4258 harbors an ADAF, it must be truncated within about 100 Schwarzschild radii (Herrnstein *et al.* 1998).

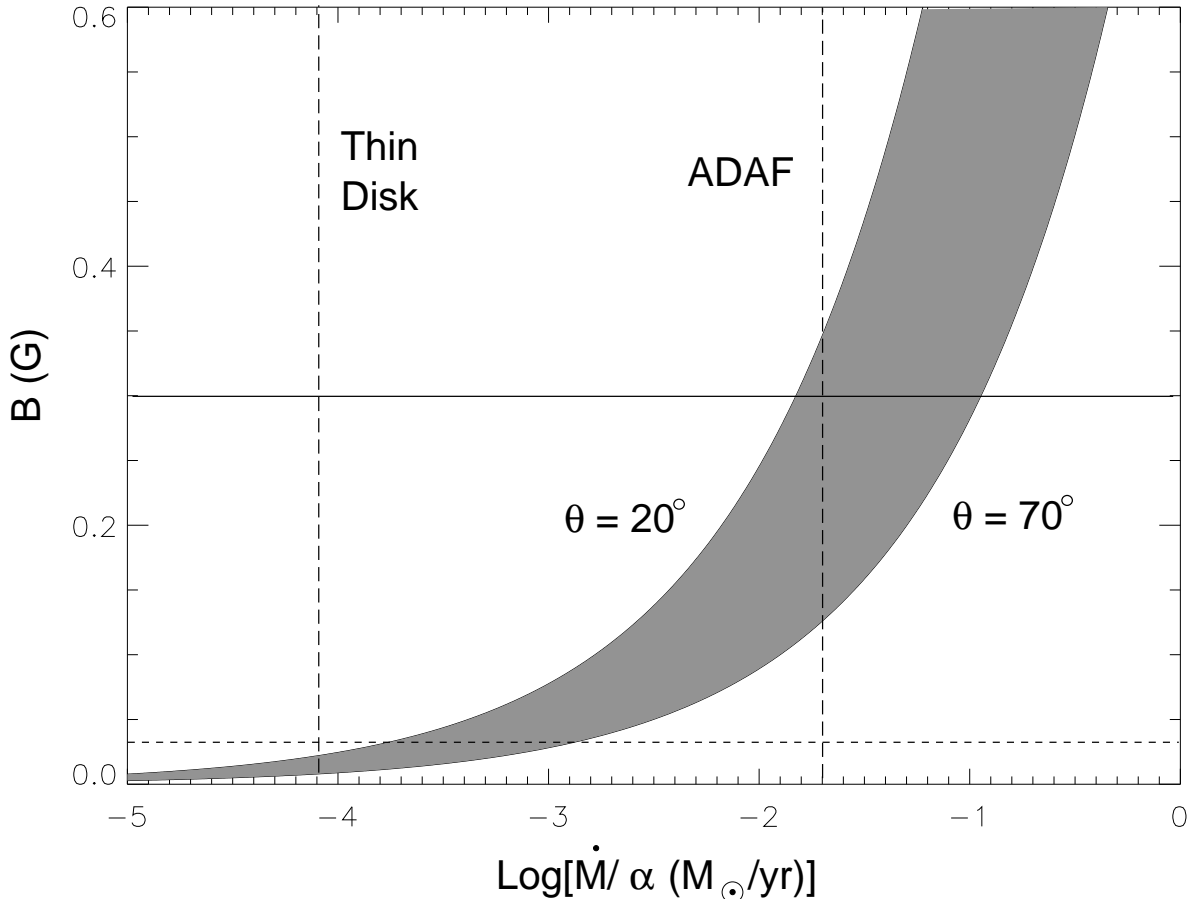


Fig. 3.— The shaded region shows the expected strength of the LOS-component of the equipartition magnetic field as a function of \dot{M}/α at a radius of 0.2 pc for a temperature of 600 K and for a range of field orientations. The accretion rates predicted by the thin-disk and ADAF models are shown (dashed vertical lines), as well as the upper limit on B_{\parallel} from the present experiment (solid horizontal line). The dashed horizontal line shows the theoretical magnetic field sensitivity of a proposed “broad-band” Zeeman experiment.

An observational determination of \dot{M} would be the most unambiguous way to discriminate between these two modes of accretion. Unfortunately, \dot{M} is very difficult to measure. The most direct constraint is derived from the extreme precision of the maser Keplerian rotation curve, and requires $\dot{M} \lesssim 10^{-1} \alpha M_{\odot} \text{yr}^{-1}$ (Herrnstein *et al.* 1998). The present upper limit on B_{\parallel} provides an additional, albeit less direct, probe of \dot{M} . Following Neufeld & Maloney (1995), we treat the X-ray-heated outer disk in NGC 4258 as a thin isothermal disk in hydrostatic equilibrium, in which the standard Shakura-Sunyaev

accretion solutions apply. The midplane pressure, p_c , is then given by (Frank, King, & Raine 1992)

$$p_c = \frac{1}{3\sqrt{2\pi^3}} \frac{GM\dot{M}}{\alpha c_s r^3}, \quad (4)$$

where M is the central mass and c_s is the isothermal sound speed. The magnetic field strength can be related to the accretion rate using equation 4 under the assumption of thermal and magnetic pressure balance in the disk ($|B|^2/8\pi = p_c$). One potential concern is that the very low ionization fraction in the molecular disk will significantly limit the coupling between the magnetic fields and the gas. However, we note that direct exposure to the central X-ray source (as a result of the warp), will generate a layer of atomic gas on top of the molecular disk with 1–2% fractional ionization, and that at $r = 0.2$ pc the molecular layer is only about 20% of the total disk thickness (Neufeld, Maloney, & Conger 1994; Herrnstein, Greenhill, & Moran 1996). The parallel component of the magnetic field is related to B according to $B_{\parallel} = uB$, where $u = \cos(\theta)$ and θ is the angle between the LOS and the magnetic field at the position of the maser in question. A disk permeated by large-scale vertical or radial fields has $u \simeq 0$ along the midline, while a disk dominated by large-scale toroidal fields has $u \simeq 1$. *Adopting a temperature of 600 K in order to accommodate the presence of masers in the disk, the present 300 mG upper limit on $|B_{\parallel}|$ together with equation 4 implies $\dot{M} \lesssim 10^{-1.9} \alpha u^{-2} M_{\odot} \text{ yr}^{-1}$.* Figure 3 shows the theoretical LOS magnetic field strength as a function of \dot{M} for $20^{\circ} < \theta < 70^{\circ}$ and illustrates that because of ambiguities in the magnetic field geometry, the present observations cannot distinguish between the ADAF and thin-disk models. We emphasize that this analysis implicitly assumes that a substantial component of the equipartition magnetic field is constant across the cross-section of the maser feature at 1306 km s^{-1} , which is thought to have a linear scale of $\sim 10^{15} \text{ cm}$ (Moran *et al.* 1995). Furthermore, the theoretical field estimates are only as accurate as the assumption of pressure balance in the disk. It is at least in principle possible to construct either thermally or magnetically dominated disk models.

While the present VLA observations are not sufficiently sensitive to discriminate between the low and high \dot{M} models, it may eventually be possible to do this by extending the Zeeman S-curve formalism to search for coherent, “broad-band” Zeeman splitting across the systemic masers, which arise on the near side of the disk (see Figure 1). In such a broad-band polarimetry experiment, one could search for a coherent frequency offset between the LCP and RCP spectra, by comparing $dI/d\nu$ to the Stokes V spectrum across the entire 100 km s^{-1} of systemic emission. Because the systemic emission is 100 times broader and 10 times brighter than the feature at 1306 km s^{-1} , the magnetic field sensitivity would be greatly enhanced. Simulations of this experiment using actual VLBA spectra

predict a 1σ uncertainty in B_{\parallel} of 30 mG, which in principle can discriminate between the low and high \dot{M} models, even accounting for ambiguities in the field configuration (dashed horizontal line in Figure 3). The broad-band Zeeman measurement would be sensitive to that component of the radial magnetic field that is constant across the systemic masers, which span about 4° in disk azimuth and 10^{16} cm in radius.

REFERENCES

- Balbus, S. A. & Hawley, J. F. 1991, *ApJ*, 376, 214
- Blandford, R. D. & Payne, D. G. 1982, *MNRAS*, 199, 883
- Braatz, J. A., Wilson, A. S., & Henkel, C. 1997, *ApJs*, 110, 231
- Cecil, G., Wilson, A. S., & De Pree 1995, *ApJ*, 440, 181
- Claussen, M. J., Heiligman, G. M., & Lo, K. Y. 1984, *Nature*, 310, 298
- Deguchi, S. & Watson, W. D. 1990, *ApJ*, 354, 649
- Deguchi, S., Nakai, N., & Barvainis, R. 1995, *AJ*, 109, 507
- Elitzur M. 1996, *ApJ*, 457, 415
- Emmering, R. T., Blandford, R. D., & Shlosman, I. 1992, *ApJ*, 385, 460
- Fiebig, D. & Gusten, R. 1989, *A&A*, 214, 333 (FG)
- Frank, J., King, A., & Raine, D. 1992, *Accretion Power in Astrophysics*, 2nd ed., Cambridge University Press
- Goldreich, P., Keeley, D. A., & Kwan, J. Y. 1973, *ApJ*, 179, 111
- Greenhill, L. G., Jiang, R. D., Moran, J. M., Reid, M. J., Lo, K. Y., & Claussen, M. J. 1995, *ApJ*, 440, 619
- Herrnstein, J. R. , Greenhill, L. J., Moran, J. M., Diamond, P. J., Inoue, M., Nakai, N., & Miyoshi, M. 1998, *ApJ*, in print
- Herrnstein, J. R. , Moran, J. M., Greenhill, L. J., Diamond, P. J., Miyoshi, M., Nakai, N., & Inoue, M. 1997, *ApJ*, 475, L17
- Herrnstein, J. R., Greenhill, L. J., & Moran, J. M. 1996, *ApJ*, 468, L17

- Lasota, J.-P., Abramowicz, M. A., Chen, X., Krolik, J., Narayan, R., & Yi, I. 1996, *ApJ*, 462, 142
- Makishima, K., Fujimoto, R., Ishisaki, Y., Kii, T., Lowenstein, M., Mushotzky, R., Serlemitsos, P., Sonobe, T., Tashiro, M., & Yaqoob, T. 1994, *Proc. Astron. Soc. Jpn.*, 46, L77
- Miyoshi, M., Moran, J. M., Herrnstein, J. R., Greenhill, L. J., Nakai, N., Diamond, P. J., & Inoue, M. 1995, *Nature*, 373, 127
- Moran, J. M., Greenhill, L. J., Herrnstein, J. R., Diamond, P. J., Miyoshi, M., Nakai, N., & Inoue, M. 1995, *Proc. Natl. Acad. Sci. USA*, **92**, 11427
- Nakai, N., Inoue, M., & Miyoshi, M. 1993, *Nature*, 361, 45
- Narayan, R. & Yi, I. 1995a, *ApJ*, 444, 231
- Narayan, R. & Yi, I. 1995b, *ApJ*, 452, 710
- Nedoluha, G. E. & Watson, W. D. 1992, *ApJ*, 384, 185
- Nedoluha, G. E. & Watson, W. D. 1991, *ApJ*, 367, L63
- Nedoluha, G. E. & Watson, W. D. 1992, *ApJ*, 361, L53
- Neufeld, D. A. & Maloney, P. R. 1995, *ApJ*, 447, L17
- Neufeld, D. A., Maloney, P. R., & Conger, S. 1994, *ApJ*, 436, L127
- Rees, M. J. 1984, *Ann. Rev. Astron. Astrophys.*, 22, 471
- Reid, M. J., & Moran, J. M. 1988, in *Galactic and Extragalactic Radio Astronomy*, ed. G. L. Verschuur & K. I. Kellermann (Berlin: Springer-Verlag), p. 255
- Shakura, N. I. & Sunyaev, R. A. 1973, *A&A*, 24, 337
- Thompson, A. R., Moran, J. M., & Swenson G. W. 1986, *Interferometry and Synthesis in Radio Astronomy*, Wiley Interscience, New York
- Wilkes, B. J., Schmidt, G. D., Smith, P. S., Mathur, S., & McLeod, K. K. 1995, *ApJ*, 455, L13
- Wallin, B. K. & Watson, W. D. 1997, *ApJ*, 481, 832
- Watson, W. D. & Wallin, B. K. 1994, *ApJ*, 432, L35

Zhao, J., Goss, W. M., & Diamond, P. J. in *Astrophysical Masers*, Springer, 1992, page 180